

# A Study for Energy-Efficient NFC-RFID Tag Antennas Used in Asset Management Applications

ALEXANDRU AVRAM, MANUELLA KADAR, ADRIAN TULBURE

Department of Informatics, Mathematics and Electronics,

“1<sup>st</sup> of December 1918” University of Alba Iulia,

Alba Iulia,

ROMANIA

*Abstract:* - The development of Near Field Communication (NFC) and Radio Frequency Identification (RFID) systems have seen significant advancements in recent years, driven by the need for secure, efficient, and interoperable solutions. This paper describes the design workflow, including theoretical backgrounds, simulations, and measurements of the passive planar antenna tags for asset management applications. According to theoretical formulations, the shape and dimensions of the antenna affect the quality of the NFC transmission because these parameters directly influence the antenna's coil inductance. We have considered two distinctive designs according to the ISO/IEC 14443 standard and the NXP Semiconductors guide for “Class 3” and “Class 6” antennas based on the NFC Forum Type 2 Tag specifications (NTAG). The optimal design results have been further used in manufacturing and validated through electrical characterization and measurements. An energy efficiency assessment has been conducted based on the proposed design and measurements. Finally, the fabricated NTAG prototype was integrated into an NFC Asset Management Application, and a conclusion and discussions on the obtained results and future development are presented.

*Key-Words:* - Energy efficiency, Antenna Theory, Antenna Design Procedure, Smart Sensor, NTAG, RFID Tag, Measurement Methods, Inventory Management.

Received: June 2, 2024. Revised: November 11, 2024. Accepted: December 4, 2024. Published: December 31, 2024.

## 1 Introduction

Near-field communication (NFC) and Radio Frequency Identification (RFID) are wireless communication technologies widely used for identification, tracking, and data exchange. Both rely on radio waves but serve different purposes and applications due to their technical characteristics, [1], [2], [3].

RFID technology enables automatic identification and tracking of objects through small, embedded tags, [1], [2]. These tags can be passive (powered by a reader's signal) or active (self-powered), making them suitable for diverse applications, [2]. RFID operates across various frequency ranges, including Low Frequency (LF) for short-range uses like animal tagging and high Frequency (HF) for applications like smart cards. RFID systems typically consist of a tag, a reader, and a backend system to process data. With ranges extending up to several meters (UHF), RFID is ideal for inventory management, access control, and toll collection.

The NFC technology, a subset of RFID, focuses on secure, short-range communication at 13.56 [MHz]. It's designed explicitly for consumer-

friendly applications, operating at a range of just a few centimeters, [3], [4]. NFC supports two-way communication, enabling tasks like contactless payments, public transport access, and device pairing. It offers three primary modes: reader/writer mode for interacting with NFC tags, peer-to-peer mode for data exchange between devices, and card emulation mode, where devices function like contactless cards.

The fundamental difference between those two lies in range and application scope. RFID excels in long-range tracking and bulk operations, while NFC prioritizes secure, close-proximity interactions, often in consumer settings. Both technologies have transformed industries, from streamlining logistics and supply chain operations with RFID to enabling cashless payments and smart device interactions through NFC, [5].

Despite their Advantages, challenges remain. RFID can be susceptible to interference and security vulnerabilities, while NFC's short-range limits its use cases. However, their adaptability and ongoing innovations continue to expand their potential in healthcare, retail, and transportation.

In summary, while RFID provides robust solutions for tracking and identification over varying distances, NFC specializes in secure, user-friendly, short-range communication, making both indispensable in modern technological ecosystems.

The new aspect of this work relies on energy efficiency measurements for optimized applications. Energy efficiency is a critical consideration in the design of NFC electronics. Modern NFC chips are equipped with energy-harvesting capabilities, allowing them to capture energy from the magnetic field generated by NFC readers. This harvested energy can be converted into an analog voltage output to power external devices such as sensors. Advanced commercial NFC chips with integrated energy-harvesting features are now readily available, enabling the creation of low-cost, energy-efficient wearable devices, [6], [7].

Moreover, the efficiency and performance of NFC systems are heavily influenced by the design, materials, and manufacturing techniques of NFC antennas. Variations in materials and fabrication methods can impact the devices' quality factor and read range. As a result, special attention must be given to optimizing NFC antenna design to ensure energy-efficient operation and enhanced device performance [5], [6].

## 2 Theoretical Backgrounds

The mathematical modeling of NFC/RFID antennas is essential to optimize their performance, ensuring maximum read range, efficient power transfer, and compatibility with the operating frequency. These models account for key parameters such as the antenna's inductance, capacitance, resistance, and resonant frequency, collectively determining the antenna's ability to resonate at the desired frequency and achieve efficient electromagnetic coupling.

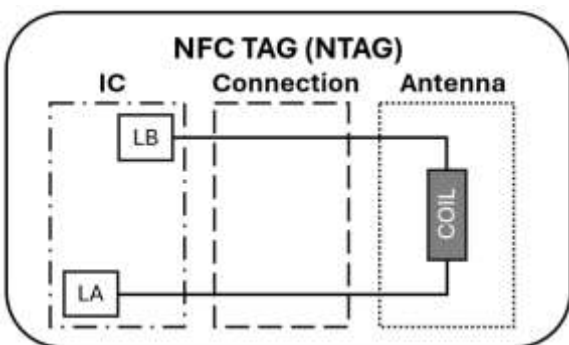


Fig. 1: Physical structure of NTAG with the electrical connection of Antenna coil terminals on LA, LB pads

Additional factors such as the antenna's geometry, inter-turn capacitance, and parasitic effects are incorporated into the models to capture real-world performance. These models guide the design process, enabling engineers to achieve an optimal trade-off between physical dimensions, manufacturing constraints, and system performance. Mathematical models often leverage circuit theory to represent NFC tag Antennas (here designed according to NXP AN11276 Application note to fully comply with ISO/IEC 14443 standard, [8], [9]) as resonant LC circuits, where the antenna's inductance  $L$  and capacitance  $C$  must balance to resonate at the operating frequency  $f_R$ .

### 2.1 Circuit Theory

Its IC must be connected to an antenna to turn the tag into an operational NFC Forum Type 2 Tag (NTAG). As represented in Fig. 1, the IC electrical connection to the Antenna is made using the LA and LB pads, [8]. The simple equivalent circuit in Fig. 2 describes the NTAG IC properties relevant to the antenna design.

The IC input capacitance  $C_{IC}$  is the most important electrical parameter of the NTAG antenna design. The manufacturer usually provides it and affects the form factor and antenna parameters.

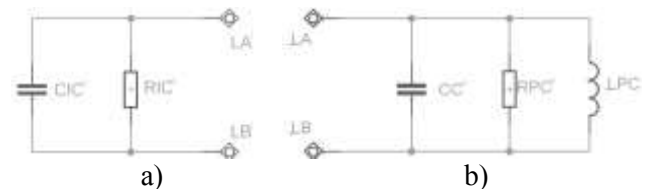


Fig. 2: The equivalent circuit of NTAG with a) the IC input capacitance  $C_{IC}$ , resistance  $R_{IC}$ , and LA, LB terminal pads, b) the Antenna capacitance  $C_C$  in parallel connection with loss resistance  $R_{pc}$  and inductance  $L_{pc}$

The antenna can be described either by an LSC inductance in series to an RSC loss resistance or by an  $L_{pc}$  inductance in parallel to an  $R_{pc}$  loss resistance.

The  $C_C$  antenna capacitance is connected in parallel to the above LR circuit (Figure 2b). This capacitance consists of inter-turn capacitance and a possibly designed tag capacitance, further detailed in section 3.1.2.

The  $R_{IC}$  input resistance of the NTAG IC (Fig. 2a), together with  $R_{pc}$  loss resistance of the antenna (Fig. 2b), and the connection resistance between these, define the tag's quality factor.

This quality factor influences the threshold field strength of the tag and can be formulated as in [8]:

$$Q_{pc} = \frac{R_{pc}}{2 \cdot \pi \cdot f_{op} \cdot L_{pc}} = Q_{sc}, \quad (1)$$

where the quality factor for parallel connection  $Q_{pc}$  is equal to the series connection  $Q_{sc}$ , and the  $L_{pc}$  and the  $R_{pc}$  terms are formulated as in [8]:

$$L_{pc} = L_{sc} \cdot \frac{1+Q_{sc}^2}{Q_{sc}^2}, \quad (2)$$

$$R_{pc} = R_{sc} \cdot (1 + Q_{sc}^2). \quad (3)$$

For further calculations, the parallel equivalent circuit in Fig. 3 was chosen to simplify the resonance circuit and its calculations, [8], [9].

In this case, the parallel equivalent capacitance of the tag can be written as in [8]:

$$C_{pl} = C_{IC} + C_{con} + C_c, \quad (4)$$

where  $C_{IC}$  is the input capacitance of the IC stated in the manufacturer's datasheet,  $C_{con}$  is the connection capacitance, and  $C_c$  is the antenna capacitance detailed in section 3.1.2.

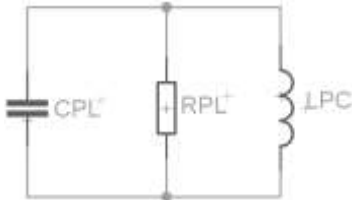


Fig. 3: Simplified parallel equivalent circuit of NTAG with the parallel equivalent capacitance  $C_{pl}$ , parallel equivalent resistance  $R_{pc}$ , and Antenna inductance  $L_{pc}$

The parallel equivalent resistance of the tag can be written as in [8]:

$$R_{pl} = \frac{R_{IC} \cdot R_{pc}}{R_{IC} + R_{pc}}, \quad (5)$$

where  $R_{IC}$  is the resistance of IC, and  $R_{pc}$  is the loss resistance of the antenna for parallel connection.

The NTAG IC's  $C_{IC}$  capacitance, the  $C_c$  antenna capacitance, and the  $C_{con}$  parasitic connection capacitance form a resonance circuit with the antenna's inductance.

## 2.2 Resonance Frequency

Based on the simplified equivalent circuit, the resonance frequency  $f_R$  of the NTAG can be calculated with the formula in [8]:

$$f_R = \frac{1}{2\pi \cdot \sqrt{L_{pc} \cdot C_{pl}}}. \quad (6)$$

## 3 Workflow Design

The design process of NFC tags depends on multiple factors, such as the system's physical properties, the environment, and the specific application. This paper presents in Fig. 4 the optimal design flowchart of NTAGs for an Asset management application.

Accurately applying the Mathematical background from the previous section ensures optimal performance and energy efficiency when designing the NTAG antenna.

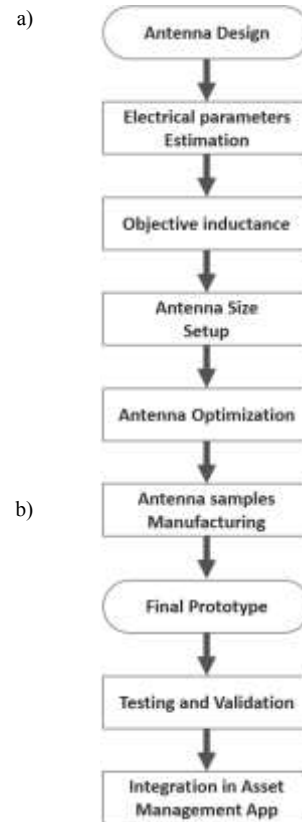


Fig. 4: The flow chart for a) design, optimization, and manufacturing process, b) validation and integration process of the NFC tag

## 3.1 Electrical Parameters

Determining the electrical parameters of the antenna tag typically involves identifying the ideal frequency, estimating the equivalent capacitance, and computing the objective inductance at which the system operates most efficiently.

The ideal threshold frequency,  $f_{IDEAL}$ , is when the tag achieves the longest read/write distance while maintaining data integrity. For a single tag operation, tuning slightly above 13.56 [MHz] would lead to maximum read/write distance.

At the resonance frequency, the parallel capacitance and antenna inductance form a resonance circuit. According to Equation (6), to compute an objective inductance, it is necessary to set the ideal frequency first and then calculate the parallel capacitance.

For this, it is necessary to estimate the  $C_c$  capacitance of the antenna in Equation (4) by using the formulation in [8]:

$$C_c = C_{it} + C_{br} + C_{in}. \quad (7)$$

The antenna capacitance can be split into the always-existing antenna inter-turn capacitance  $C_{it}$ , the additional capacitance due to possibly realized bridge  $C_{br}$ , and a possible designed on-tag capacitance  $C_{in}$ .

The antenna inter-turn capacitance  $C_{it}$  depends upon the technology used for the antenna manufacturing (Wired, Etched, or Printed). In contrast, the capacitance of a possibly realized bridge  $C_{br}$  depends on the bridge length and width.

### 3.2 Objective Inductance

Setting the ideal threshold frequency  $f_{IDEAL}$  and computing the parallel equivalent capacitance  $C_{pl}$ , the objective inductance  $L_o$  can be further calculated for design purposes, as in [8]:

$$L_o = \frac{1}{(2\pi \cdot f_{IDEAL})^2 \cdot C_{pl}} \quad (8)$$

### 3.3 Antenna Size Setup

This section provides the procedure for the development of rectangular antenna types. The inductance for this type of antenna can be written as in [8] based on geometrical parameters:

$$L_{calc} = \frac{\mu_0}{\pi} \cdot [x_1 + x_2 - x_3 + x_4] \cdot N_c^2, \quad (9)$$

with  $x_1$ ,  $x_2$ ,  $x_3$ , and  $x_4$  as terms depending on  $a_{avg}$ ,  $b_{avg}$ , the average dimensions of the antenna, as in [8]:

$$a_{avg} = a_o - N_c \cdot (g + w), \quad (10)$$

$$b_{avg} = b_o - N_c \cdot (g + w), \quad (11)$$

where  $a_o$ ,  $b_o$  are the overall dimensions of the antenna,  $w$  is the track width,  $g$  the gap between the tracks and  $N_c$  is the number of turns.

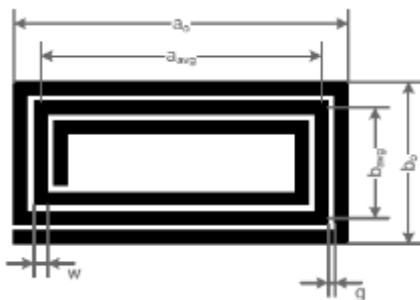


Fig. 5: Rectangular antenna design parameters with:  $a_o$ ,  $b_o$  is the overall dimensions of the antenna,  $w$  is the track width, and  $g$  the gap between the tracks, as in [8]

The maximum dimensions of the antenna in Figure 5,  $a_{max}$  and  $b_{max}$ , are determined by the application for which the tag is designed. Therefore,

the starting point for the calculations is always  $a_o = a_{max}$  and  $b_o = b_{max}$ .

The antenna production process defines the minimal gap between the tracks  $g_{min}$ . To get the highest possible antenna area,  $g = g_{min}$ .

It is recommended that the track width be not too small, as it influences the quality factor  $Q_{pc}$  in Equation (1). The track width remains the fit parameter for calculating the inductance  $L_{calc}$  in Equation (9).

Under the assumption that all turns are concentrated on the outline of the antenna, all magnetic flux passes the enclosed area of all turns (no stray field), and the magnetic coupling between the turns is 100%, the inductance is proportional to  $N_c^2$ .

### 3.4 Antenna Optimization

The optimization process usually implies trial-and-error procedure. To decide which antenna best fits the resonance frequency requirements, measuring the tag resonance frequency and comparing it with the ideal frequency previously defined is usually recommended. A prototype of the designed antenna may be used for this. Due to the high costs of manpower and time, a simulation procedure is recommended instead for optimization purposes.

By modeling the antenna geometry and incorporating parameters such as the number of turns, trace width, spacing, and substrate properties into computer-aided Engineering (CAE) software, one can numerically solve equations or use equivalent circuit models to estimate the antenna's inductance. The results from the Simulation software are compared against the computed inductance to identify discrepancies, refine the design, and ensure that the antenna resonates at the desired frequency.

For choosing the best antenna, calculate the difference between the measured/simulated resonance frequency  $f_R$  and the ideal resonance frequency  $f_{ideal}$  using:

$$\Delta f_{ideal-R} = |f_{ideal} - f_R|. \quad (12)$$

The optimum antenna is the antenna that's nearest to  $f_{ideal}$ ,  $\Delta f_{ideal-R} = \min$ . Usually, the antenna chosen here is the final one for NTAG designs.

NXP Semiconductors also provides datasheets and procedures for optimizing the correlation of Electrical and Dimensional parameters for NTAG antennas based on the ISO/IEC 14443 standard, [10].

Results section 4 details the Final prototype and Manufacturing from Figure 12, as well as Testing and validation by measurement procedures, Simulations, and equipment.

## 4 Results

According to the NXP Semiconductors guide [8] and the ISO/IEC 14443 standard [9], six antenna classes (Class 1—Class 6) are defined. All six classes describe different form factors and sizes. NXP recommends using the Class 3—Class 6 antennas for an NFC tag, [8].

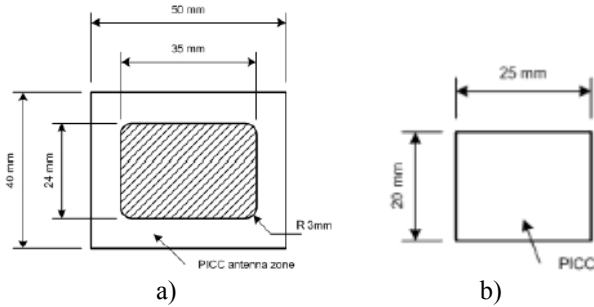


Fig. 6: Antenna classes definition according to NXP guide [8] with a) “Class 3” and b) “Class 6” antenna type and dimensional limitations

In this work, two different designs were considered for “Class 3” and “Class 6” antennas based on the NFC Forum Type 2 Tag specifications (NTAG).

The “Class 3” antenna shall be located within a zone defined either by an external rectangle of 50 x 40 [mm] or by an internal rectangle of 35 x 24 [mm], centered in the external rectangle, with a 3 [mm] corner radius, Fig. 6a). The “Class 6” antenna design shall be located within a zone defined by a rectangle of dimensions 25 x 20 [mm], Fig. 6b).

### 4.1 Materials and Methods

The design process of planar antennas is a crucial stage in the development of modern communication systems. As described in section 3, the antenna design starts with determining the electrical parameters of the tag antenna.

Firstly, the ideal threshold frequency  $f_{IDEAL} = 14.5$  [MHz] is set slightly above the 13.56 [MHz] resonance frequency to achieve the longest read/write distance.

Then, the  $L_o$  objective inductance should be calculated using Equation (8). The  $C_{pl}$  capacitance in Equation (4) must first be computed to calculate this inductance.

For this, the NTAG213F type IC from NXP was considered, with  $C_{IC}$  capacitance of 50 [pF] at  $V_{LA-LB} = 1.5$  [Vrms] and  $f_R = 13.56$  [MHz] measuring conditions, according to [8]. Then, the  $C_{Con}$  connection capacitance was estimated in the 0.5–2 [pF] range, as in [8]. Lastly, the  $C_c$  antenna capacitance was calculated using Equation (7).

Here, the  $C_{it}$  antenna inter-turn capacitance was first estimated in the 2–4 [pF] range, considering the Etching technology used for the antenna manufacturing. Then, the  $C_{br}$  capacitance of a possibly realized bridge was estimated based on the bridge length and width in the 1–5 [pF] range.

Considering the above information, the total  $C_{pIT}$  parallel capacitance of the proposed NTAG is finally estimated at 55 [pF].

The  $L_o$  objective inductance is computed at 2.19 [ $\mu$ H]. To keep the value of the aim inductance around 2.1 [ $\mu$ H] (with 10% tolerance) while resonance frequency varies with distance within the 13.5–14.5 [MHz] range, we used a tuning capacitance up to 15 [pF].

The Printed Circuit Board (PCB) layout design for a tag's planar antenna (Fig. 7), following the inductance computation in Equation (9), involves translating the dimensional parameters from section 3.3 into a physical layout that meets electrical and manufacturing requirements. The PCB rectangular structure consists of an FR4 dielectric support with  $E_r = 4.3$  relative permittivity and double-layered etched copper wire materials designed using Altium Design software.

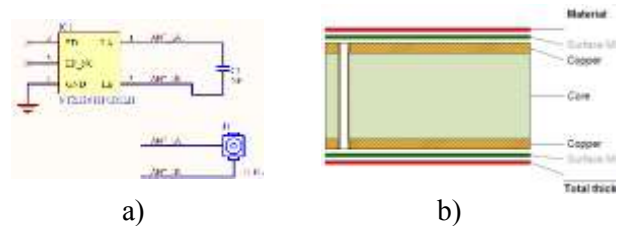


Fig. 7: The PCB layout for both selected Class 3 and 6 antennae with a) the Schematic circuit and b) stack-up layers

To achieve the optimal antenna designs, physical parameters such as trace width, inter-turn spacing, and total loop area were optimized according to section 3.4.

Table 1. Physical parameters and dimensions for “Class 3” and “Class 6” antenna

Shape	Class	Length [mm]	Width [mm]	Turns N	Width [μm]	Spacing [μm]	Height [μm]
Rectangle	3	43	32	5	300	300	35
Rectangle	6	25	20	7	250	100	35

At the end of the optimization process, the Copper track thickness  $t = 35$  [ $\mu$ m] was selected, and the track width  $w$  in the 250–300 [ $\mu$ m] range was recommended to not influence the quality factor  $Q_{pc}$

in Equation (1). The gap  $g$  between the tracks of 100 [ $\mu\text{m}$ ] for the “Class 3”, and 300 [ $\mu\text{m}$ ] for the “Class 6” antenna was setup.

The turn exponent  $p$  was estimated in the 1.75-1.85 range, corresponding to Etching manufacturing technology.

Table 1 presents the physical parameters for “Class 3” and “Class 6” antenna.

In Fig. 8, the “Class 3” antenna design output after optimization is presented.

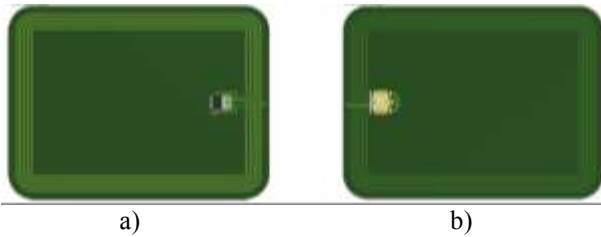


Fig. 8: The realistic view of PCB antenna layout with a) Top view with IC and tuning, b) Bottom view with U.FL connector for “Class 3” antenna type

Potential issues, such as power losses or interference, can be quickly identified by simulating the antenna's behavior before the design's physical implementation. This reduces development time and enhances the system's final performance.

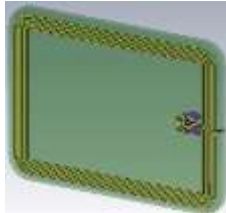


Fig. 9: The 3D CAD model of “Class 3” antenna exported from Altium

CST Design Studio provides a powerful platform for simulating the inductance of a tag planar antenna, enabling the theoretical computations to be validated.

The 3D mechanical CAD model in Fig. 9 was exported from Altium to the CSD Design software to simulate the electrical parameters of the optimal designs.

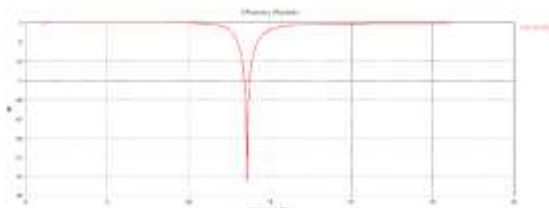


Fig. 10: Simulated  $S_{11}$  parameters for the “Class 3” antenna design, with resonance frequency at 14.5 MHz

The simulated S parameters (Fig. 10) result shows a resonant frequency  $f_R$  of 14.5 MHz for the optimized “Class 3” antenna type, as verified by Equation (12).

The simulated inductance of  $L_{11}=2.1$  [ $\mu\text{H}$ ] as results in Fig. 11 is validated by  $L_o=2.19$  [ $\mu\text{H}$ ] computed objective inductance.

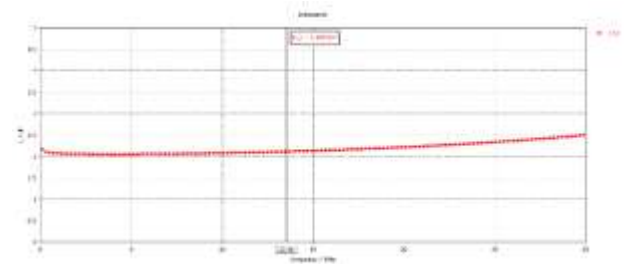


Fig. 11: Simulated inductance  $L_{11}$  for “Class 3” antenna design, at resonance frequency of 13.56 MHz

## 4.2 Final Prototypes

The manufactured PCB (Fig. 12) utilizes an FR4 substrate with a 1.59 [mm] thickness, providing the necessary mechanical stability and optimal performance in the RFID operating environment. The board is equipped with copper traces of 35 [ $\mu\text{m}$ ] thickness, enabling efficient conductivity and minimizing signal losses, essential for fast and reliable communication between the tag and the reader. These specifications are chosen to meet the performance requirements of NTAG tags, which operate at a frequency of 13.56 [MHz], ensuring a balance between cost, reliability, and energy efficiency.



Fig. 12: Final PCB antenna products according to NXP “Class 3” and “Class 6” populated with a) IC and tuning capacitor on top, b) U.FL connector on the bottom.

The top and bottom sides were masked according to ISO/IEC 14443 standards and populated with surface-mounted technology (SMT) according to the PCB Schematic and layout (Fig. 8).

## 4.3 Measurement Results

The equivalent circuit of the antenna was determined using measuring instruments (Impedance analyzer,

Network/ Spectrum analyzer, LCR meter) with associated measuring principles. As in [11], a short calibration was performed with this measurement antenna connected to the instrument's terminals.

Measuring the inductance of a planar antenna is a critical step in validating the design against theoretical calculations and simulations. This process ensures that the manufactured antenna meets the intended specifications and performs optimally within the RFID system.

The Hioki Impedance Analyzer was connected to the antenna without an IC, and the inductance was measured. Results in Figure 13 show an inductance of  $L_p=2.04$  [ $\mu\text{H}$ ] that is validated by the computed  $L_o$  value in Equation (8) and the simulated inductance  $L_{11}$  in Fig. 11.



Fig. 13: Measurements of parallel RCL components of Class 3 antenna using the Impedance Analyzer

Keysight Vector Network Analyzer E5061B (Figure 14a) achieved characterization and validation. To evaluate the parallel RCL equivalent circuit of the NTAG with IC, a user-defined fixture (Figure 14b) of an N-type to SMA port adapter and an 8[mm] SMA to U.FL cable connector was manufactured.

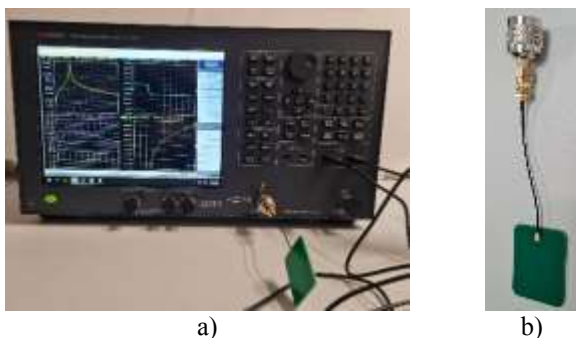


Fig. 14: Measurements setup for parallel RCL components of Class 3 antenna with a) Keysight VNA and b) User-defined fixture on Port 1

During the calibration procedure, cables and adapters were compensated for any interference with measurement results. The Reflection method on VNA Port 1 results (Fig. 15a shows a phase shift at  $f_R = 12.5$  [MHz] resonant frequency and  $Z$  impedance amplitude at 9.9 [k $\Omega$ ] for this circuit.

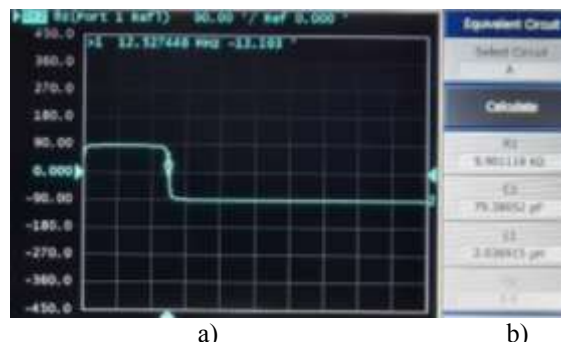


Fig. 15: Measurement results of a) phase shift and b) parallel RCL components of "Class 3" antenna at the resonance frequency

The parallel RCL equivalent circuit results in Fig. 15b show an inductance of  $L_1=2.04$  [ $\mu\text{H}$ ] at 12.5 [MHz] operating frequency, validated by the  $L_o$  computed and  $L_{11}$  simulated inductance values. The measured capacitance  $C_1 = 79.3$  [pF] consists of  $C_{p1} = 55$  [pF] computed capacitance plus a tuning capacitor of 15 [pF] and resulted in on-tag capacitance  $C_{in}$ .

The measurements setup for the energy-efficiency study consists of an RC522 RFID module connected to an Analog Discovery digital oscilloscope (Figure 16). To measure the power consumption in Sleeping mode, the reading distance range was varied between 0 and 5 cm (Table 2).

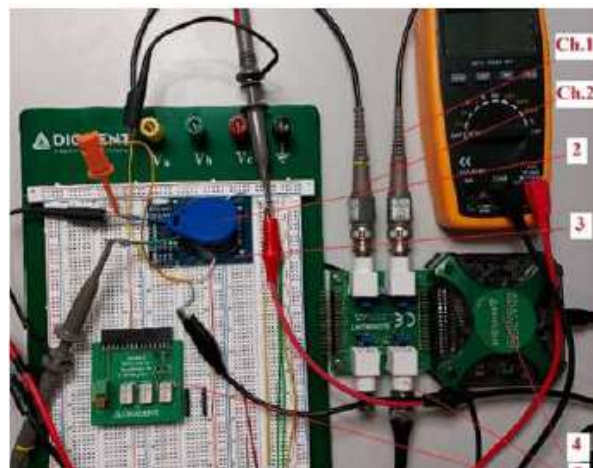


Fig. 16: Measurements setup for energy-efficiency of RFID systems

Measurement results for the NFC antenna demonstrate that the tag's dimensions directly influence the reading distance.

The smaller NTAG "Class 6" antenna achieves a reading distance of up to 1.5 [cm], while the more prominent "Class 3" antenna extends the reading distance to 3 [cm].

Table 2. Measurements comparison of the reading range energy between Class 3 and Class 6 antenna tags

Reading range [cm]	Sleep mode Class 3 [mW]	Sleep mode Class 6 [mW]
1	126	85
3	32	-
5	2	-

#### 4.4 Integration into Asset Management App

The Asset Management App is a software solution designed to help organizations track, manage, and optimize the use of their physical and digital assets throughout their lifecycle.

The Asset Management System, obtained by pairing the fabricated NTAGs with the TagWriter Mobile App by NXP, offers an efficient solution for tagging, tracking, and managing assets using NFC technology. The system lets users write and encode data onto NFC tags attached to physical assets, such as equipment, inventory, or documents.

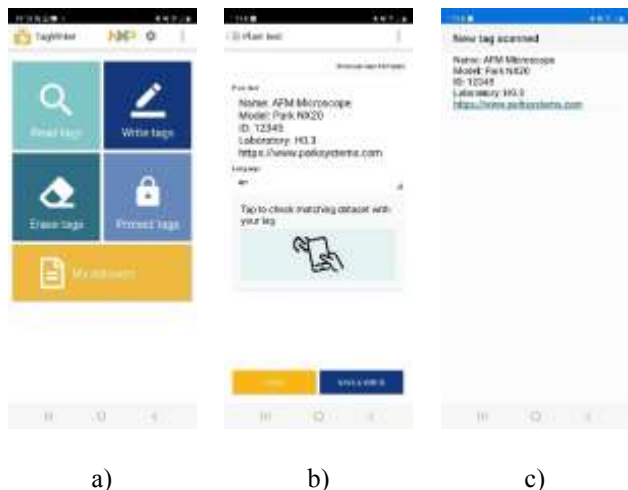


Fig. 17: Generic Architecture of the Asset Management App

The generic App architecture is presented in Fig. 17. The NXP TagWriter application loaded the database inventory based on .csv files. The information from the database was written into the Class 3 and Class 6 NTAGs and visualized on the mobile phone display.

#### 5 Conclusion and Future Work

This study demonstrated that the shape and dimensions of NFC-RFID antennas affect data transmission quality. The physical parameters directly influence the antenna’s coil inductance. Two

distinctive designs were considered according to the ISO/IEC 14443 standard and the NXP Semiconductors guide for “Class 3” and “Class 6” antennas based on the NFC Forum Type 2 Tag specifications (NTAG).

The optimal design resulted in a validated prototype that was ready for manufacturing and tested in the Asset Management App.

The study highlights the critical relationship between the dimensional parameters and shape of NFC passive tags and their energy efficiency in enabling communication.

The study’s results underline the correlation between tag size and reading distance, indicating that larger antennas are more energy-efficient in harvesting and transmitting signals over extended distances. This relationship is vital to balancing compactness and operational performance based on specific application requirements.

The Asset Management App facilitates easy data input, customization, and encoding NTAG directly from a smartphone, ensuring quick deployment.

#### Acknowledgment:

The authors acknowledge the financial support provided by Research Contract No. 870/25.09.2024, concluded between the University of Alba Iulia and Infogrup SRL.

#### Declaration of Generative AI and AI-assisted Technologies in the Writing Process

The authors wrote, reviewed and edited the content as needed and they have not utilised artificial intelligence (AI) tools. The authors take full responsibility for the content of the publication.

#### References:

- [1] Costa F, Genovesi S, Borgese M, Michel A, Dicandia FA, Manara G. A review of RFID sensors, the new frontier of Internet of things. *Sensors*. 2021; 21(9):3138. <https://doi.org/10.3390/s21093138>.
- [2] El Gaabouri I, Senhadji M, Belkasmi M, El Bhiri B. A Systematic Literature Review on Authentication and Threat Challenges on RFID Based NFC Applications. *Future Internet* 2023; 15(11):354. <https://doi.org/10.3390/fi15110354>.
- [3] Cao Z, Chen P, Ma Z, Li S, Gao X, Wu R-x, Pan L, Shi Y. Near-Field Communication Sensors. *Sensors*. 2019; 19(18):3947. <https://doi.org/10.3390/s19183947>.

- [4] Coskun, V., Ozdenizci, B. & Ok, K. A Survey on Near Field Communication (NFC) Technology. *Wireless Pers Commun* **71**, 2259–2294 (2013). <https://doi.org/10.1007/s11277-012-0935-5>.
- [5] Lazaro A, Villarino R, Girbau D. A Survey of NFC Sensors Based on Energy Harvesting for IoT Applications. *Sensors* (Basel). 2018 Nov 2;18(11):3746. doi: 10.3390/s18113746.
- [6] J. Victoria, A. Suarez, P. A. Martinez, A. Alcarria, A. Gerfer and J. Torres, "Improving the Efficiency of NFC Systems Through Optimizing the Sintered Ferrite Sheet Thickness Selection," in *IEEE Transactions on Electromagnetic Compatibility*, vol. 62, no. 4, pp. 1504-1514. doi: 10.1109/TEMC.2020.3003800.
- [7] M. -A. Chung, Y. -L. Chien, L. Cho, P. -H. Hsu and C. -F. Yang, "A dual-mode antenna for wireless charging and Near Field Communication," *2015 IEEE International Symposium on Antennas and Propagation & USNC/URSI National Radio Science Meeting*, Vancouver, BC, Canada, 2015, pp. 1288-1289, doi: 10.1109/APS.2015.7305033.
- [8] AN11276 NTAG Antenna Design Guide - Application note, BU-ID Doc. No.: 2421, [Online]. [https://www.google.com/url?sa=t&source=web&rct=j&opi=89978449&url=https://community.nxp.com/pwmx87654/attachments/pwmx87654/nfc/6155/1/AN11276.pdf&ved=2ahUKEw iZ7cTskcOLAxUAQfEDHdi4LRYQFnoECB8QAQ&usg=AOvVaw2P0BW\\_jSxt2vCT30TcIQ8](https://www.google.com/url?sa=t&source=web&rct=j&opi=89978449&url=https://community.nxp.com/pwmx87654/attachments/pwmx87654/nfc/6155/1/AN11276.pdf&ved=2ahUKEw iZ7cTskcOLAxUAQfEDHdi4LRYQFnoECB8QAQ&usg=AOvVaw2P0BW_jSxt2vCT30TcIQ8) (Accessed Date: October 10, 2024).
- [9] ISO/IEC 14443-1:2018, Cards and security devices for personal identification — Contactless proximity objects, Part 1: Physical characteristics, [Online]. <https://www.iso.org/standard/73596.html> (Accessed Date: October 10, 2024).
- [10] NTAG213\_215\_216, NFC Forum Type 2 Tag compliant IC with 144/504/888 bytes user memory [Online]. [https://www.nxp.com/docs/en/data-sheet/NTAG213\\_215\\_216.pdf](https://www.nxp.com/docs/en/data-sheet/NTAG213_215_216.pdf) (Accessed Date: October 10, 2024).
- [11] B. ȚEBREAN, C. MUREȘAN and T. E. CRIȘAN, "Acquisition and Monitoring System for Basic Laboratory Measurements on Electrical Networks Parameters," *2023 10th International Conference on Modern Power Systems (MPS)*, Cluj-Napoca, Romania, 2023, pp. 1-4, doi: 10.1109/MPS58874.2023.10187478.

### **Contribution of Individual Authors to the Creation of a Scientific Article (Ghostwriting Policy)**

The authors equally contributed in the present research, at all stages from the formulation of the problem to the final findings and solution.

### **Sources of Funding for Research Presented in a Scientific Article or Scientific Article Itself**

No funding was received for conducting this study.

### **Conflict of Interest**

The authors have no conflicts of interest to declare.

### **Creative Commons Attribution License 4.0 (Attribution 4.0 International, CC BY 4.0)**

This article is published under the terms of the Creative Commons Attribution License 4.0

[https://creativecommons.org/licenses/by/4.0/deed.en\\_US](https://creativecommons.org/licenses/by/4.0/deed.en_US)